# Modeling spectral changes following stimulation:

# Is there an event-related shift in 1/*f* activity?

Máté Gyurkovics[1], Grace M. Clements[1,2], Kathy A. Low[1], Monica Fabiani[1,2],
& Gabriele Gratton[1,2*]

[1] Beckman Institute, University of Illinois at Urbana-Champaign, IL, 61801, USA

[2] Psychology Department, University of Illinois at Urbana-Champaign, IL, 61820, USA

**Abbreviated title**: EVENT-RELATED SPECTRAL CHANGE

*** Correspondence:**

Prof. Gabriele Gratton

grattong@illinois.edu

Dr. Máté Gyurkovics

mate.gyurkovics@gmail.com

## Abstract

Neural activity contains oscillatory components (i.e., narrowband oscillations) and non-oscillatory components (e.g., event-related potentials [ERPs] and 1/*f*-like background activity). Here, surface-level EEG data was analyzed to investigate how the spectral content of neural activity below 25 Hz changes from before to after an event. We focused on changes in non-oscillatory background activity, a spectral component often assumed to be static across time in time-frequency analyses. During a simple auditory perception task (n = 46) and an auditory oddball task (n = 23), we found an apparent increase in the offset and a decrease in the slope of 1/*f* activity from before to after a tone. Importantly, however, these changes in non-oscillatory background activity were almost completely accounted for by the emergence of ERPs in response to the stimulus in frequencies below the alpha range (8-12 Hz). Our findings suggest that post-event spectral changes below 25 Hz can be modelled as the sum of pre-event non-oscillatory activity, the spectrum of the ERP, and an independent alpha component that is modulated in amplitude, but not elicited, by the event. Theta activity (4-8 Hz), however, was not present before the event and appeared to be phase-locked to it. The theoretical and methodological implications of our findings regarding the nature and origin of 1/*f* activity, and the interpretation of low-frequency activity in the time-frequency domain are discussed.



**Key words**: 1/*f* activity, ERP, alpha power, theta power, power spectrum

## 1. Introduction

Neural activity, as measured by electromagnetic methods such as EEG and MEG, can be divided into two broad classes: oscillatory activity and non-oscillatory, aperiodic activity. In M/EEG recordings, oscillatory activity refers to rhythmic changes in the activation of a set of neurons, which repeat over time in a predictable fashion, with consistent shape and duration (Cohen, 2014b). Oscillations can be seen as increased power in a narrow frequency band in the frequency or time-frequency domain representations of neural data (Cohen, 2014b; Donoghue et al., 2020; Herrmann et al., 2014). Canonical frequency bands of interest include the delta (0.5-4 Hz), theta (4-8 Hz), alpha (8-12 Hz), beta (12-30 Hz), and gamma (>30 Hz) ranges. Notably, activity in these frequency bands has been linked to a wide variety of sensory and cognitive processes in the literature (Başar et al., 2000; Buzsáki, 2002; Clayton et al., 2015; Cohen, 2014a; Lundqvist et al., 2016; Mathewson et al., 2011). In terms of its generative mechanism, oscillatory activity in M/EEG likely reflects the activity of thalamo-cortical and cortico-cortical feedback loops (Cohen, 2014b; Gratton, 2018; Pfurtscheller & Da Silva, 1999).

Non-oscillatory activity, instead, refers to changes in neuronal activation that do not repeat predictably over time, or at all, and are therefore aperiodic. There are two types of aperiodic activity commonly observed in M/EEG recordings: event-related potentials (ERPs) and 1/*f*-like aperiodic activity (or 1/*f* activity for short). ERPs capture synchronized, transient changes in the post-synaptic potentials of large groups of similarly aligned cortical neurons, which occur time-locked to an eliciting event, e.g., the presentation of a stimulus (Luck, 2014). It has been called into question whether ERPs are truly aperiodic, and argued that they reflect ongoing oscillations whose phases are reset to the same value on each trial by the stimulus, creating phase-locked activity, which then emerges as an ERP following time-domain averaging (Makeig et al., 2002). It is possible that both mechanisms are present at the same time, and that ERPs could result from the emergence of a transient signal that is added

to ongoing neural activity, as well as the partial reset of the phase of ongoing oscillations, especially in the alpha band (Min et al., 2007; Mishra et al., 2012; Sauseng et al., 2007). As such, ERPs may be considered to reflect aperiodic activity as well as the event-related reorganization of periodic activity.

The second type of aperiodic activity is reflected in the shape of the power (or amplitude) spectrum of electrophysiological signals in the frequency domain. Typically, power in such signals decreases as a function of frequency, following a power law of the form $1/f^x$, where $f$ denotes frequency and $x$ is an exponent that determines the steepness of the drop-off in power across frequencies (He, 2014; He et al., 2010; Pritchard, 1992; Voytek & Knight, 2015); hence the term $1/f$ activity. This broadband property of the power spectrum is hypothesized to reflect ongoing non-oscillatory activity, as opposed to narrow-band oscillations, which manifest as "bumps" atop the $1/f$ scaling (Donoghue et al., 2020). It should be noted, however, that $1/f$ activity is present whenever there is some form of autocorrelation in a particular signal, but this autocorrelation does not correspond to a rhythmic phenomenon (e.g., when autocorrelation is due to deflections of variable duration occurring at random times in a time series). Nevertheless, changes in the shape of $1/f$ activity in the brain have been linked to shifts in the balance between excitatory and inhibitory synaptic inputs in local neural circuits (Gao et al., 2017). Furthermore, although $1/f$ activity is often regarded as noise to be excluded before performing frequency-domain analyses (Gyurkovics et al., 2021), the shape parameters of $1/f$ activity have been found to be related to behavior and cognition (Bódizs et al., 2021; Clements, Bowie, et al., 2021; Immink et al., 2021; Lendner et al., 2020; Ouyang et al., 2020).

Both internal and external events can lead to changes in an electrophysiological time series. ERPs reflect transient changes *elicited* by such events and, as mentioned earlier, they may also reflect phase-locked, oscillatory activity elicited or phase-reset by an event. An

event may also *induce* non-phase-locked changes in the amplitude of ongoing oscillatory activity, which is most readily observed with time-frequency analysis (Cohen, 2014b; Herrmann et al., 2014; Pfurtscheller & Da Silva, 1999). All these changes, however, occur against the backdrop of ubiquitous 1/*f* activity. However, thus far in surface level M/EEG recordings it has not been systematically investigated whether aperiodic, 1/*f*-like background activity changes in response to an event, and if yes, what factors might account for this change.

It is reasonable to assume that 1/*f* activity may change in response to external events, because the slope (*x*) and offset of 1/*f* activity have both been found to change as a function of neuronal activation levels in local brain activity measured by invasive recordings (Miller et al., 2009; Podvalny et al., 2015). Recently, 1/*f* activity has also been shown to be sensitive to the balance between excitatory and inhibitory neural activity in surface EEG recordings, which reflect activity summated over larger areas of the cortex as opposed to local activity (Waschke et al., 2021), and this balance might also change during tasks. Furthermore, M/EEG findings by Wainio-Theberge et al. (2021) suggest that the parameters describing the shape of pre-stimulus and post-stimulus 1/*f* activity may in fact differ, although that study did not directly investigate this question.

Within this context, it is also important to note that some common techniques used in the analysis of oscillatory signals, such as time-frequency analysis, implicitly assume that 1/*f* activity remains stable throughout an epoch, and control for this background activity based on this assumption, to avoid confounding estimates of oscillatory activity. Specifically, background activity is assumed to remain unchanged from the pre-stimulus period to the post-stimulus period, meaning that it can be corrected for by removing – either through division or subtraction (Gyurkovics et al., 2021) – a pre-stimulus estimate of 1/*f* activity from the whole epoch to isolate the oscillatory activities of interest (Cohen, 2014b; Herrmann et al., 2014). If,

however, the level of aperiodic 1/*f* activity changes in response to stimuli or responses, in a manner similar to induced changes in oscillatory activity, then this correction method rests on a problematic assumption.

In the present study, we tested the tenability of this core analytic assumption, by investigating if stimulus-related changes can be detected in 1/*f* activity in surface EEG in a simple perceptual task and an oddball task in the auditory modality. Both tasks had jittered inter-trial intervals (ITIs) of at least 5 s, ensuring that a) stimulus onset was never predictable, b) spectral changes elicited by stimulus N-1 had time to subside before stimulus N, and c) there was sufficient time both pre- and post-stimulus to estimate activity in frequency ranges below theta (< 4 Hz). Furthermore, we also explored whether any observed changes in non-oscillatory (i.e., aperiodic) activity from before to after stimulus presentation could be accounted for by the addition of ERP activity to the unchanged background activity. Note, however, that we expect stimuli to also induce a change in oscillatory activity, e.g., in the form of alpha suppression, and that ERP activity would not be expected to account for this oscillatory change. Therefore, we investigated whether the post-stimulus spectrum could be accurately predicted from the sum of the pre-stimulus spectrum and the spectrum of the ERP (at frequencies outside of the alpha range), or whether there are broadband changes not captured by this simple two-predictor model (e.g., a shift in non-oscillatory background activity).

Notably, for any frequency range where post-stimulus power can be modelled as the sum of pre-stimulus power and the power of the ERP, we would need to conclude that the ERP does not include phase-locked oscillations of that particular frequency. If it did, the sum of the pre-stimulus power spectrum and the ERP power spectrum should systematically exceed the actual post-stimulus spectrum. This is because this oscillatory activity would be represented twice in the synthesized spectra obtained by adding the pre-stimulus and ERP

spectra. In this sense, the data would also be relevant to the question of whether ERP activity is, to a significant extent, due to phase resetting of oscillatory activity outside the alpha range.

In summary, the present study investigated the following questions: 1) Is there a difference in the shape parameters of 1/*f* (aperiodic) activity in the EEG signal from before to after stimulation? 2) If yes, what is the relationship between the spectrum of the ERP generated by the stimulus and the change in 1/*f* parameters occurring from before to after stimulation? Finally, 3) can we model the post-event spectrum as the sum of the ERP spectrum and a continuation of the aperiodic activity observed before the presentation of the stimuli in most frequency ranges?

## 2. Method

### 2.1 Participants

Two samples collected for a different project (described in Clements, Gyurkovics, et al., 2021) were re-analyzed for the current study. Sample 1 consisted of 34 young and 12 older adults ($n_{total}$ = 46, mean age = 35 ± 22.2, 56.5% female) who completed a simple auditory perception task (described in detail in Section 2.2). Sample 2 consisted of a subsample of the younger adults from Sample 1 (n = 23, mean age = 22 ± 2.5, 60.9% female), who completed an auditory oddball task (described in detail in Section 2.2) in a separate session.

### 2.2 Stimuli and Procedure

Participants in Sample 1 completed 3 blocks of rest: with eyes open, with eyes closed, and with eyes open but wearing a mask covering their eyes, and 3 blocks with identical eye status conditions, but with the addition of random tone sounds (pips). A 75-ms long, 500 Hz sinusoidal tone was used as the pip, and it was played binaurally from two speakers outside the participant's field of vision. Participants were told that they would hear pips, but they did not have to respond to them in any form (passive task). There were 25 pips in each block,

with randomly jittered inter-stimulus intervals between 5 and 10 s. Each block lasted approximately 2-3 minutes. The order of the different types of blocks (eyes open, eyes closed, or masked; rest or pips) was counterbalanced across participants. Only data from the eyes open pip condition were used in the current study. Participants had to maintain fixation on a cross presented at the center of a computer monitor throughout the block in this condition.

Participants in Sample 2 completed 12 blocks of an auditory oddball task, 6 with eyes open and 6 with eyes closed, counterbalanced across participants in groups of 3 (e.g., 3 eyes open, 3 eyes closed, 3 eyes open, 3 eyes closed). Participants heard 25 pips per block (total = 300). However, approximately 20% of the pips (rare pips, on average 60 trials) differed in pitch from the other 80% (frequent pips, on average 240 trials). Which pip (450 Hz or 500 Hz) was assigned to the rare and frequent group was counterbalanced across participants. All pips were 75 ms in duration. Participants were instructed to mentally count the rare pips and report their number at the end of each block. No other response was required. ISIs were 5-10 s, similarly to the previous task. Only data from the eyes open blocks was used in the current study.

In the oddball task, trials were sorted into three conditions based on the trial sequence (Clements, Gyurkovics, et al., 2021) to control for well-established sequential effects in oddball paradigms (Brumback et al., 2005). The conditions were: frequent pips preceded by another frequent pip (frequent-frequent, approximately 64% of trials), frequent pips preceded by a rare pip (rare-frequent, approximately 16% of trials), and rare pips preceded by a frequent pip (frequent-rare, approximately 16% of trials). The first pip in each block was discarded from analysis as it had no previous trial type information, and so were rare pips preceded by other rare pips as this trial type occurred extremely infrequently (on approximately 4% of trials).

## 2.3 EEG Recording and Pre-processing

The EEG and electrooculogram (EOG) were recorded from 64 electrodes (60 EEG electrodes placed according to an extended 10-20 system (Acharya et al., 2016; Jasper, 1958), and 4 EOG electrodes placed above and below the right eye, and 2 cm outside the outer canthi of each eye) during rest and while the participants completed the tasks, using a BrainAmp (BrainVision Products GmbH) recording system. EOG and EEG were recorded with a sampling rate of 500 Hz referenced to the left mastoid on-line. The EEG was subsequently re-referenced to the average of the left and right mastoids off-line; vertical and horizontal EOG derivations were obtained by subtracting the below-eye channel from the above-eye channel, and the right-eye channel from the left-eye channel, respectively. Impedance was kept below 10kΩ during recording. Online, the data were filtered with a 0.5-200 Hz bandpass. Offline, data were pre-processed using the EEGLAB Toolbox (version: 13.6.5, Delorme & Makeig, 2004) and custom MATLAB 2019b scripts (The MathWorks Inc., Natick, MA, USA). A 30 Hz low-pass filter was applied. EEG and EOG data were then segmented into 5120 ms (2560 points) long epochs around pip onset (-2558 ms to 2560 ms, with the onset of the pip being 0 ms). Any EEG channel with variance at least 100 times larger than the median variance of all other EEG channels was considered a bad channel and interpolated as the mean of surrounding good channels. Epochs with amplifier saturation were excluded from further analysis. Vertical (blinks) and horizontal (saccades) ocular artifacts were corrected using the procedure described in Gratton et al. (1983), based on the eye channel recordings. Finally, all epochs with voltage fluctuations at any EEG channel exceeding 200 $\mu$V after eye movement correction were discarded.

To verify that pips were successfully presented, they were recorded via two separate circuits connected to the speakers. They were recorded using V-Amp (BrainVision Products GmbH) with a 1-200 Hz online bandpass filter and 500 Hz sampling rate.

For the frequency analysis of event-related changes in $1/f$ scaling, the pre-event window was defined as the 1024-ms (512 points) long window immediately preceding the onset of the stimulus (-1022 to time point 0), and the post-event window as the 1024-ms (512 points) long window immediately after stimulus onset (2 ms to 1024 ms). The Fourier transform of activity in these time windows was taken on each trial at each electrode for every subject, using MATLAB's built-in fft() function. No padding was used, as the epoch lengths expressed in time points were a power of 2. Spectral resolution was 1/1.024 Hz (0.977 Hz). The resulting power spectra were then averaged across trials for the two windows separately within each participant. Frequencies below 1.95 Hz and above 25.39 Hz were removed from further analysis. Then, the resulting spectra were decomposed into oscillatory (periodic) and non-oscillatory (aperiodic) components in semi-log space, using the FOOOF algorithm (v1.0.0, Donoghue et al. , 2020)[1]. The aperiodic component of a frequency-domain signal represents $1/f$ activity in the absence of any narrowband oscillations, and the offset and slope (exponent) of this component were estimated for each spectrum. $1/f$ activity (the aperiodic component) at each electrode for each subject, before and after the event, was then reconstructed in linear space as $10^{(ß + x\log10(f))}$ where $ß$ is the offset in log space, $f$ is frequency, and $x$ is the slope of the curve. The offset value in linear space ($10^{ß}$), the slope (with a negative sign, i.e., $x$), and the reconstructed aperiodic component in each time window, at each electrode for every participant were retained for future analyses, along with the central frequency of each oscillatory bump identified by the FOOOF algorithm. Post- minus pre-event differences were also computed for the offset, the slope, and the aperiodic component of the modeled spectrum.

To characterize event-related changes in the frequency domain, the power spectrum of the ERP at each electrode was also saved, calculated by taking the Fourier transform of the

[1] The following settings were used for spectral parametrization: peak_width_limits=[2,8], max_n_peaks=6, min_peak_height=0.1, peak_threshold=2.0, aperiodic_mode='fixed'.

time-domain average of post-event window activity across trials. The offset, slope, and estimated aperiodic component of these spectra were also determined, in an identical manner to the one described above. The rationale for isolating the aperiodic component of the spectrum of the ERP was that, as noted in the Introduction, some activity phase-locked to an event may be oscillatory in nature, which could show up as peaks in the spectrum of the ERP. The grand mean ERP spectra (shown in Fig. 3B) confirmed that, in general, the frequency domain representation of this signal contained both narrowband peaks and a broadband component where power decreased across frequencies. Notably, however, it was an open empirical question whether this latter component could be fit by a $1/f$ curve.

A critical question in this paper is whether the post-stimulus power spectrum can be accurately predicted by adding the ERP power spectrum to the pre-stimulus power spectrum. However, even in the absence of a stimulus, there might be a difference between the power spectra for consecutive epochs due to random moment-to-moment fluctuations. Therefore, as a control, we compared the accuracy of predicting the post-event spectrum based on the sum of the pre-event and ERP spectra, to the accuracy of predicting the power spectrum of one second of data from that of the previous second in the absence of stimulation. Specifically, we contrasted the spectrum of the 1024 ms (512 points) time window immediately preceding the stimulus (which we label the “event-1 window”, and is identical to the pre-event window in the previous analyses) and a 1024 ms (512 points) time window immediately preceding this event-1 window (which we label the “event-2 window”). Note that, due to the long intertrial intervals, no event could occur within less than 5000 ms of any other event. As such, we considered that this event-2/event-1 comparison captured non-event related fluctuations in spectral content which could occur in the absence of stimulation. Also note that to make the comparison completely symmetric to the summed spectrum used to predict the post-stimulus spectrum, we also generated a summed spectrum obtained by adding the event-2 spectrum

and the spectrum of the average event-1 EEG traces (which we label "pseudo-ERP"). Although expected to be negligible in power, this latter spectrum is nevertheless unlikely to be flat since power is always positive, and therefore its contribution should not be ignored. In sum, this additional control comparison should generate an "unbiased" benchmark to which event-related changes in the shape of the spectrum could be compared.

**2.4 Statistical Analysis**

All statistical analyses were based on non-parametric methods, using a truncated permutation distribution approach. First, we tested whether there is an overall significant difference, across all electrodes, between the pre- and post-event offset and slope estimates of the $1/f$ component of the spectrum, as computed using FOOOF. To this end, the grand mean post-minus-pre difference value across all electrodes and all participants was compared against a null distribution of difference values based on 10,000 permutations, separately for each parameter (offset and slope). On each permutation, the sign of the cross-electrode mean difference for a given parameter was flipped for a random half of the subjects, and the grand mean difference was calculated on this new sample. This resulted in a null distribution with 10,000 grand mean values, in which the $2.5^{th}$ and $97.5^{th}$ percentiles were identified. If the observed grand mean difference value fell outside of the range between these two percentiles, it was considered significant at $p < .05$ (two-tailed). In Sample 2, this procedure was run separately for each condition. Note that the different conditions had different trial numbers in Sample 2; therefore results across conditions should not be directly compared. We elected not to equalize the number of trials across conditions to preserve as much statistical power as possible and because cross-condition differences were of no relevance to our research question.

Based on the scalp distribution of parameter differences in Sample 1, a midline subset of electrodes (Fz, F1, F2, FCz, FC1, FC2, Cz, C1, C2, CPz, CP1, CP2, Pz, P1, P2, see Figure 1

insets) was identified as a primary region of interest, and all subsequent analyses were conducted on the average of these electrodes.

Next, we investigated whether post-event changes in the aperiodic component of the power spectrum (i.e., in $1/f$ activity, reconstructed based on parameters provided by FOOOF) could be accounted for by the emergence of ERPs. We calculated how accurately the pre-event aperiodic component, the aperiodic component of the ERP spectrum, and the combination of these two predictors predict the post-event aperiodic component within the electrode subset of interest for each participant separately, by simply subtracting either the pre-event aperiodic component, the ERP aperiodic component, or both from the post-event aperiodic component. This resulted in three sets of subtraction-based residuals across frequencies for each participant. Residuals were then normalized by the post-event aperiodic component to account for the decrease in mean power and variance across frequencies. The normalized values were then squared and averaged across participants, separately for each of the three sets of residuals. The resulting proportional prediction error values were then examined to determine how well different predictors account for post-event aperiodic content. The best fitting model – i.e., the model with the lowest proportional prediction errors – was then contrasted against the identical model based on the event-2 pre-event aperiodic component predicting the event-1 pre-event component. This was done to determine whether there is variance unaccounted for by our model of choice in the post-event aperiodic component, above and beyond random moment-to-moment spectral variability (as captured by the event-2/event-1 control analyses).

Identical analyses were also conducted on the raw spectra, i.e., before spectral parametrization by FOOOF. Note that in these analyses, post-event reductions in narrowband power, e.g., in the alpha range, cannot be predicted by either pre-event power or by adding the power obtained before the stimulus and the power of the ERP at that frequency, since power

can never be less than 0. Therefore, for some frequencies, the normalization process might result in proportional error values greater than 1.

## 3. Results

Pre-processing and analysis code for all analyses can be found at the following URL: https://osf.io/nq8jk/.

### 3.1. 1/*f* Offset Increases and Slope Decreases After an Event.

As a reminder, we are asking whether: 1) there is a difference in the shape parameters of 1/*f* (aperiodic) activity in the EEG signal (as estimated by FOOOF) from before to after stimulation. 2) If yes, we aim to determine the relationship between the spectrum of the ERP generated by the stimulus and the change in 1/*f* parameters occurring from before to after stimulation Finally, 3) we will investigate if the post-event spectrum can be modelled as the sum of the ERP spectrum plus a continuation of the aperiodic activity observed before the presentation of the stimuli in most frequency ranges.

Figures 1A and 1B present data relevant to the first question. These plots compare the observed changes in 1/*f* parameters (solid vertical lines, offset: Figure 1A; slope: Figure 1B) after stimulation (i.e., differences in these parameters when applying FOOOF to the spectra of the post-event vs. event-1 windows) with histograms showing the permutation-based null distribution of these parameters. For these analyses, the parameters were averaged across all electrodes and participants, but kept separate for the four conditions (passive stimulation from Sample 1 and the three oddball conditions from Sample 2). For each null distribution, the 2.5$^{th}$ and 97.5$^{th}$ percentiles are marked with dashed vertical lines. In all cases, the observed grand mean offset difference value is higher than the 97.5$^{th}$ percentile cut-off, suggesting that averaged across all electrodes, 1/*f* activity had a higher offset following the stimulus compared to immediately before the stimulus. Conversely, the observed grand mean slope

difference value is negative, and below the 2.5$^{th}$ percentile in all cases. This suggests that, in general, the slope of 1/*f* activity was steeper (more negative) following the stimulus compared to before the stimulus. The insets show the scalp distribution of the observed parameter differences. They indicate that pre- post-differences in offset were maximal at frontocentral electrodes in most conditions, whereas slope difference had a broader scalp distribution.

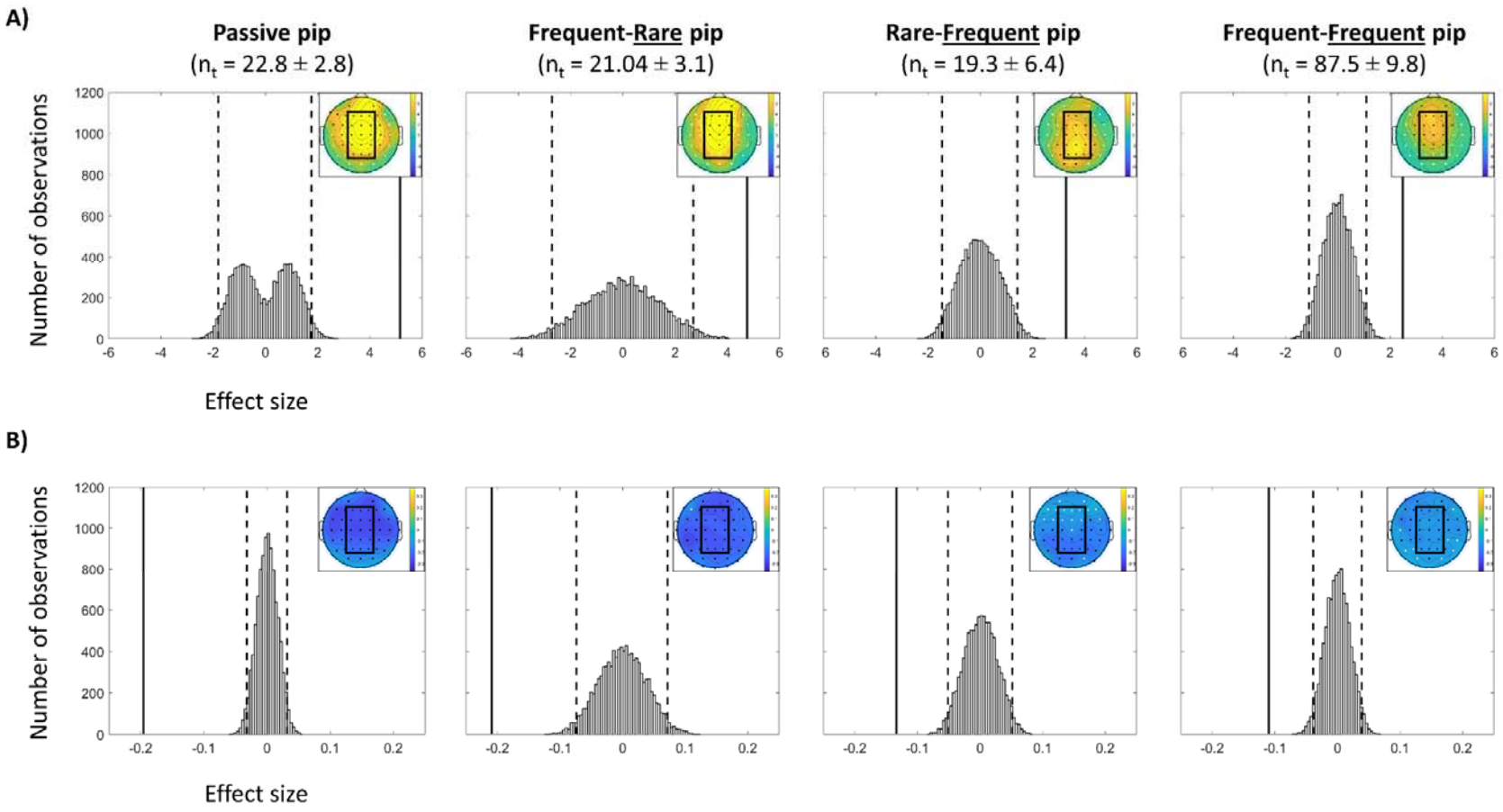
A)
Passive pip
($n_t$ = 22.8 ± 2.8)
Frequent-Rare pip
($n_t$ = 21.04 ± 3.1)
Rare-Frequent pip
($n_t$ = 19.3 ± 6.4)
Frequent-Frequent pip
($n_t$ = 87.5 ± 9.8)
Number of observations
Effect size
B)
Number of observations
Effect size

**Figure 1** - Differences in the parameters of 1/*f* activity from pre- to post-event time windows across different conditions. Trial numbers differ across conditions, $n_t$ = mean trial numbers ± SD. A) Permutation testing the mean post-event minus pre-event offset difference value across four conditions. In each panel, the vertical black line is the observed mean offset difference across all electrodes and participants. The distribution is the permutation-based null distribution, with the $2.5^{th}$ and the $97.5^{th}$ percentiles marked by dashed lines. Please note that the bimodal distribution in the passive pip condition suggests the presence of an outlier. Removing this outlier does not change the results appreciably, although it does rectify the shape of the null distribution. Insets show the scalp distribution of the post-event minus pre-event offset differences, averaged across participants. Electrodes marked in black are significant compared to a null distribution of extreme values based on permutation testing. Units are arbitrary (AU). The black rectangle indicates the subset of electrodes used in all subsequent analyses. B) Same as A but for the exponent parameter.

To ensure relative comparability across samples and conditions, a midfrontal subset of electrodes (marked by the black rectangles in Fig. 1) was identified, and all further analyses were based on average activity across electrodes within this subset (see Section 2.4 for further details). Fig. 2A shows the estimated aperiodic components (1/*f* activity) of the pre-event and post-event spectra, based on the parameters estimated by FOOOF, averaged across electrodes of interest, and participants. Fig. 2B shows the raw spectra before FOOOF decomposition for these time windows. These figures illustrate the shift in 1/*f* activity from pre- to post-event, which was also illustrated by the parameter changes shown in Fig. 1. Furthermore, Fig. 2B also reveals oscillatory changes from pre- to post-event, most clearly post-event suppression in the alpha range, and, in some cases, a post-event increase in the theta range.

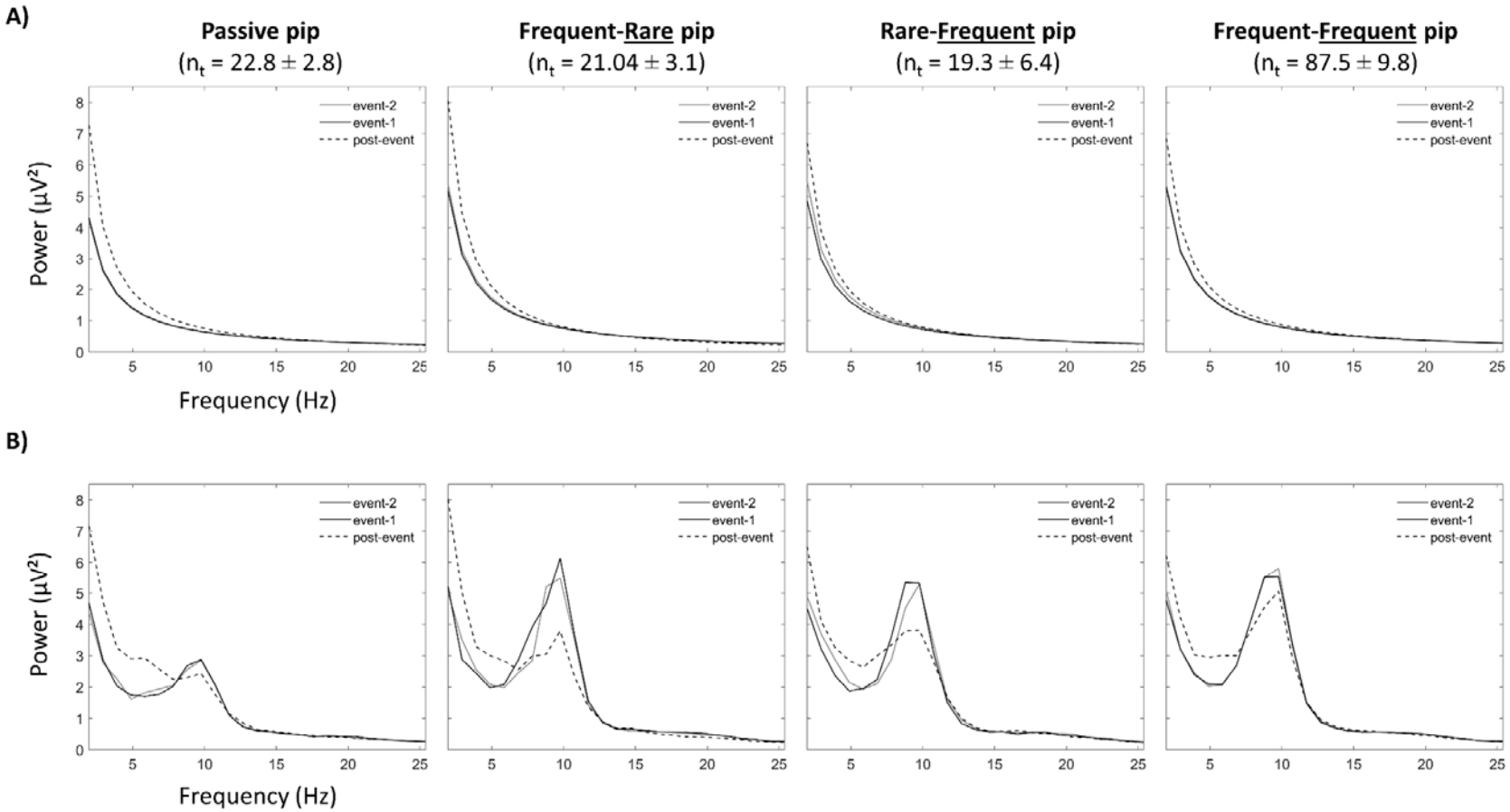
A)
Passive pip
($n_t$ = 22.8 ± 2.8)
Frequent-Rare pip
($n_t$ = 21.04 ± 3.1)
Rare-Frequent pip
($n_t$ = 19.3 ± 6.4)
Frequent-Frequent pip
($n_t$ = 87.5 ± 9.8)
event-2
event-1
post-event
Power (μV²)
Frequency (Hz)
B)
event-2
event-1
post-event
Power (μV²)
Frequency (Hz)

367

**Figure 2** - Pre- and post-event spectral content in the midfrontal electrode subset of interest. Averaged across participants. Trial numbers differ across conditions, $n_t$ = mean trial numbers ± SD. A) Pre- and post-event aperiodic components across the four conditions, reconstructed based on the parameters estimated provided by FOOOF. Post-event refers to 1 to 1025 ms after the target tone (pip), event-1 (or pre-event) refers to -1024 to 0 ms, and event-2 refers to -2049 to -1025. B) Same as A but with the raw spectra.

Figure 3 provides a qualitative summary of findings relevant to the second question, concerning the relationship of the spectrum of the ERP to post-event spectral changes. The spectrum of the ERP refers to the frequency-domain representation of the time-domain average of post-event activity. Figure 3A shows the comparison between the shape of the post- minus pre-event difference in aperiodic components modeled using FOOOF parameters and the reconstructed aperiodic portion of the ERP spectrum in each condition. Fig. 3B shows the post- minus pre-event difference in the raw spectra, along with the raw spectra of the ERPs. In both rows, ERP spectral content below the alpha range is qualitatively similar to the post-minus-pre difference spectra – albeit less so for the estimated aperiodic component than for the raw spectra. This may be because the estimation of the $1/f$ curve was substantially noisier for the spectrum of the ERP (which is based on a single epoch, averaged in the time-domain) than for the other two spectra (which are based on the average of multiple spectra across trials). Noise in estimation for different conditions is illustrated in Supp. Fig. 1. This raised concerns about the comparability of aperiodic estimates for the ERP spectra with those of all other spectra. Consequently, we decided to focus only on the raw spectra, containing both $1/f$ activity and oscillatory peaks, in further analyses. Findings based on estimated aperiodic components can be found in the *supplementary materials* (Supp. Figs. 2 and 3). The results are largely similar across these two sets of analyses, although the impact of increased noise in estimation is clear in the aperiodic component findings, especially at lower frequencies

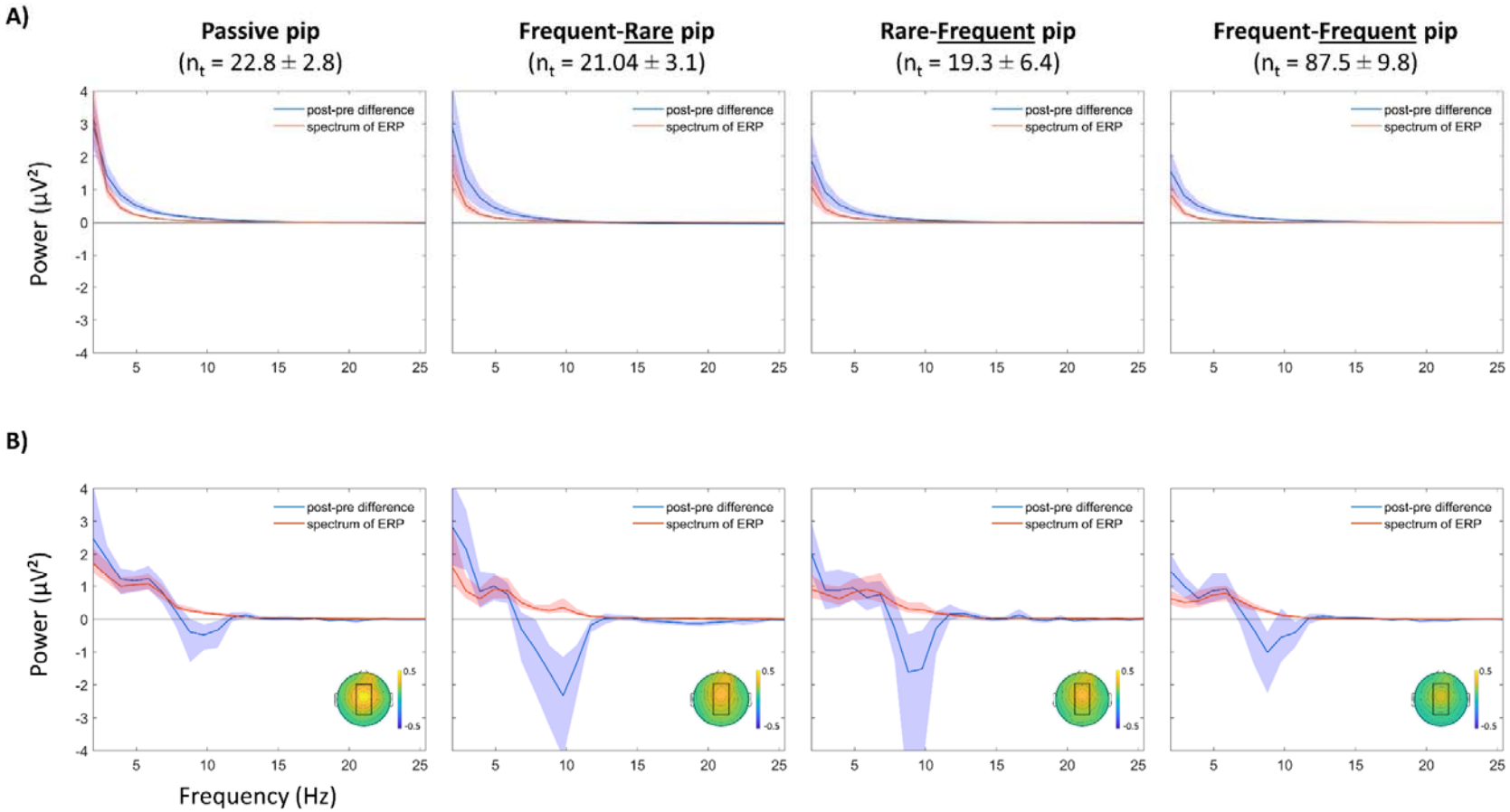
A)
Passive pip
($n_t$ = 22.8 ± 2.8)
Frequent-Rare pip
($n_t$ = 21.04 ± 3.1)
Rare-Frequent pip
($n_t$ = 19.3 ± 6.4)
Frequent-Frequent pip
($n_t$ = 87.5 ± 9.8)
post-pre difference
spectrum of ERP
Power (μV²)
B)
Frequency (Hz)

**Figure 3** – Event-related differences in spectral content across different conditions. Trial numbers differ across conditions, $n_t$ = mean trial numbers ± SD. A) The average post- minus pre-event difference in aperiodic components (where pre-event refers to event-1), and the aperiodic component of the ERPs (activity averaged in the time-domain in the post-event window) across conditions. Shading is 95% bootstrapped confidence interval. B) Same as A but using raw spectra. Insets show the scalp distribution of global ERP power in $\mu V^2$ . ERP = event-related potential.

The difference spectra in Fig. 3 highlight a clear shift in 1/*f* activity (manifested as a broadband change in low-frequency activity in the raw spectra). The raw spectrum of the ERP also shows a non-linearity (bump) in the theta range (4-8 Hz) similar to the raw post-event spectrum (Fig 2B, see also Supp. Fig. 4 for a traditional analysis of post-event phase locking). This observation is supported by the distribution of the central frequencies of each oscillatory peak recovered by FOOOF. Supp. Fig. 5 shows the distribution of the frequency of each identified peak, across all electrodes and participants. While alpha activity is prominent in both the pre-event and post-event windows, peaks in the theta range were most frequently identified in the post-event and the ERP spectra, although increased noise makes the interpretation of the latter estimates less straightforward, as noted above.

In summary, the data indicate that FOOOF-estimated parameters of 1/*f*-like background activity differ from before to after auditory stimulation. Furthermore, there is notable similarity between the observed change in the shape of the spectrum from pre- to post-event and the spectrum of the ERPs.

**3.2. Broadband Changes in the Power Spectrum Are Largely Due to ERPs**.

The remainder of the analyses were designed to address the third question of our study: Can we model the post-stimulus spectrum as the sum of ongoing aperiodic activity and the ERP spectrum? To address this question, we formally investigated how well the spectral content of the ERPs could account for post-event changes in the frequency spectrum, using the raw spectra instead of the reconstructed aperiodic components, for the reasons noted above. Specifically, we used the sum of the pre-event and ERP spectra of each participant to predict their corresponding post-event spectrum (two-predictor model). We also compared this model with simpler models using only the pre-event spectrum or the spectrum of the ERP as predictors (one-predictor models). Mean prediction errors, expressed as a proportion of power in the to-be-predicted post-event window for each frequency, are shown in Fig. 4A for

the different conditions. These plots reveal three clear patterns: 1) the ERP spectrum on its own yields an extremely poor fit, especially at higher frequencies, 2) prediction errors are typically high in the alpha range even for the pre-event-only and the two-predictor models, because neither of those can account for alpha suppression, or indeed, any type of suppression in oscillatory activity, and 3) outside of the alpha range, the proportional prediction error curves for these latter two models are largely flat and do not show a $1/f$-like shape (with a non-zero exponent).

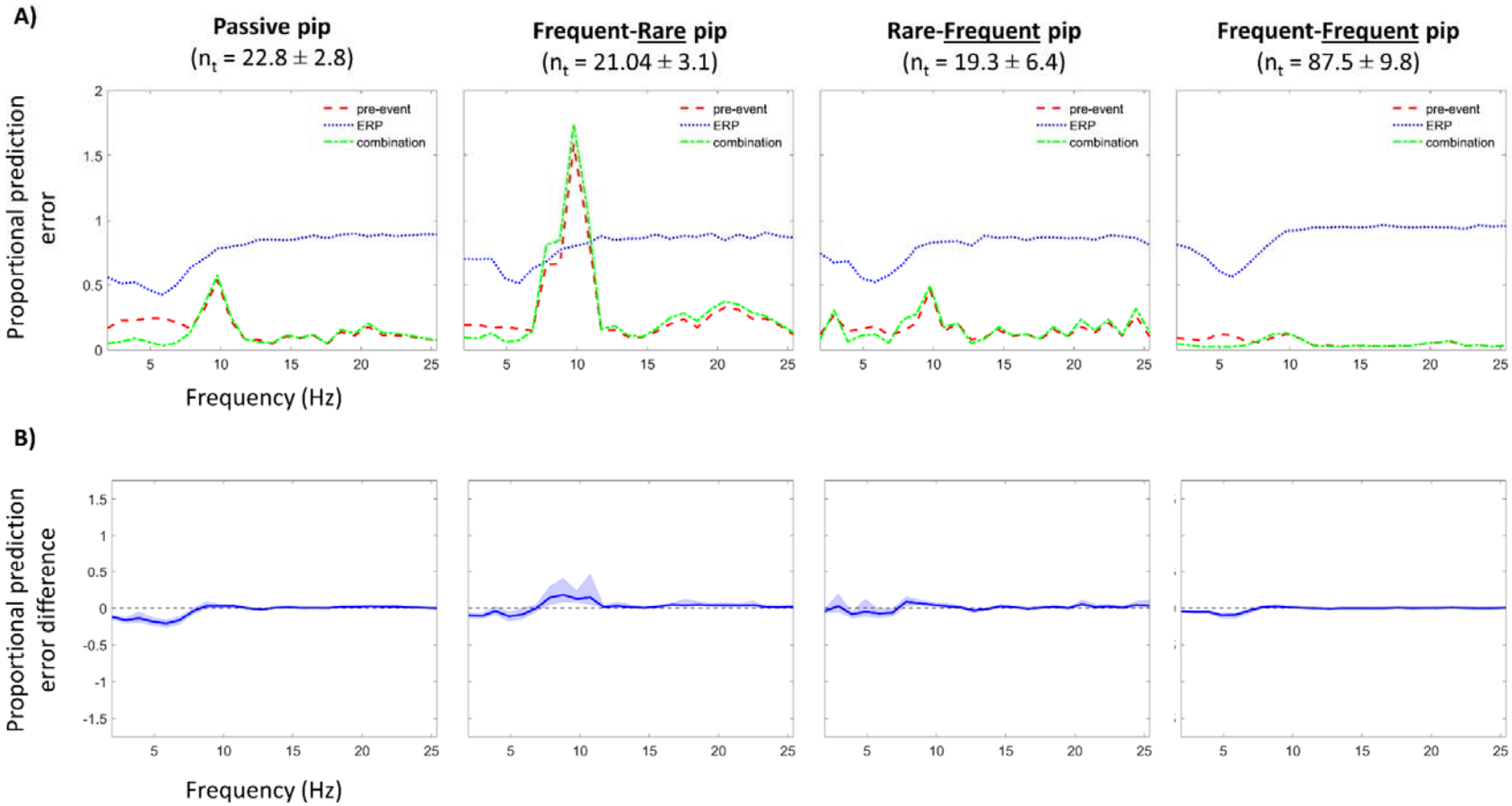
A)
Passive pip
($n_t$ = 22.8 ± 2.8)
Frequent-Rare pip
($n_t$ = 21.04 ± 3.1)
Rare-Frequent pip
($n_t$ = 19.3 ± 6.4)
Frequent-Frequent pip
($n_t$ = 87.5 ± 9.8)
pre-event
ERP
combination
Proportional prediction error
Frequency (Hz)
B)
Proportional prediction error difference
Frequency (Hz)

431
432

**Figure 4** – Frequency-wise proportional prediction errors across different conditions. Trial numbers differ across conditions, $n_t$ = mean trial numbers ± SD. A) Prediction errors expressed as a proportion of the power in the post-event spectrum, using three different sets of predictors: the pre-event (event-1) spectrum on its own (red), the spectrum of the ERP on its own (blue), and the two predictors together (two-predictor model, green). The outcome was always the post-event spectrum. Values are averaged across individuals. B) The difference between the two-predictor model and the pre-event only model error curves (the green and red lines from Row A, respectively). Shading is 95% bootstrapped confidence interval. ERP = event-related potential.

To statistically assess these qualitative patterns, we compared the prediction error for the pre-event-only (one-predictor) model to the prediction error for the two-predictor model (pre-event + ERP). The mean difference (two-predictor minus one-predictor) between the two proportional error curves is shown in Fig. 4B, with a 95% bootstrapped confidence interval for each frequency. Based on these plots, both models perform with similar accuracy, but prediction errors tend to be lower for the two-predictor model than the one predictor model at low frequencies, suggesting that accounting for the spectral content of the ERPs improves the fit of ongoing aperiodic activity to post-event spectral content.

Note, however, that some residual error remains. Next, we examined whether this error reflected unexplained variance above and beyond measurement error. Measurement error was quantified as the prediction error between the spectra of two adjacent time windows – event-2 and event-1 - in the absence of stimulation, i.e., error that likely occurs simply due to random, moment-to-moment variability in the spectral composition of the signal (see Section 2.4). Fig. 5A shows the proportional prediction error curves for the two-predictor model from Fig. 4 (“event” scenario) along with measurement error curves based on the event-2 and event-1 windows (“no event” scenario; see Fig. 2 for the power spectra in these two non-event-related windows). Fig. 5B shows the mean difference between these two curves (event minus no event) for each condition, along with the 95% bootstrapped CI. These figures indicate no systematic differences between the event and no-event scenarios in terms of prediction accuracy outside the alpha range.

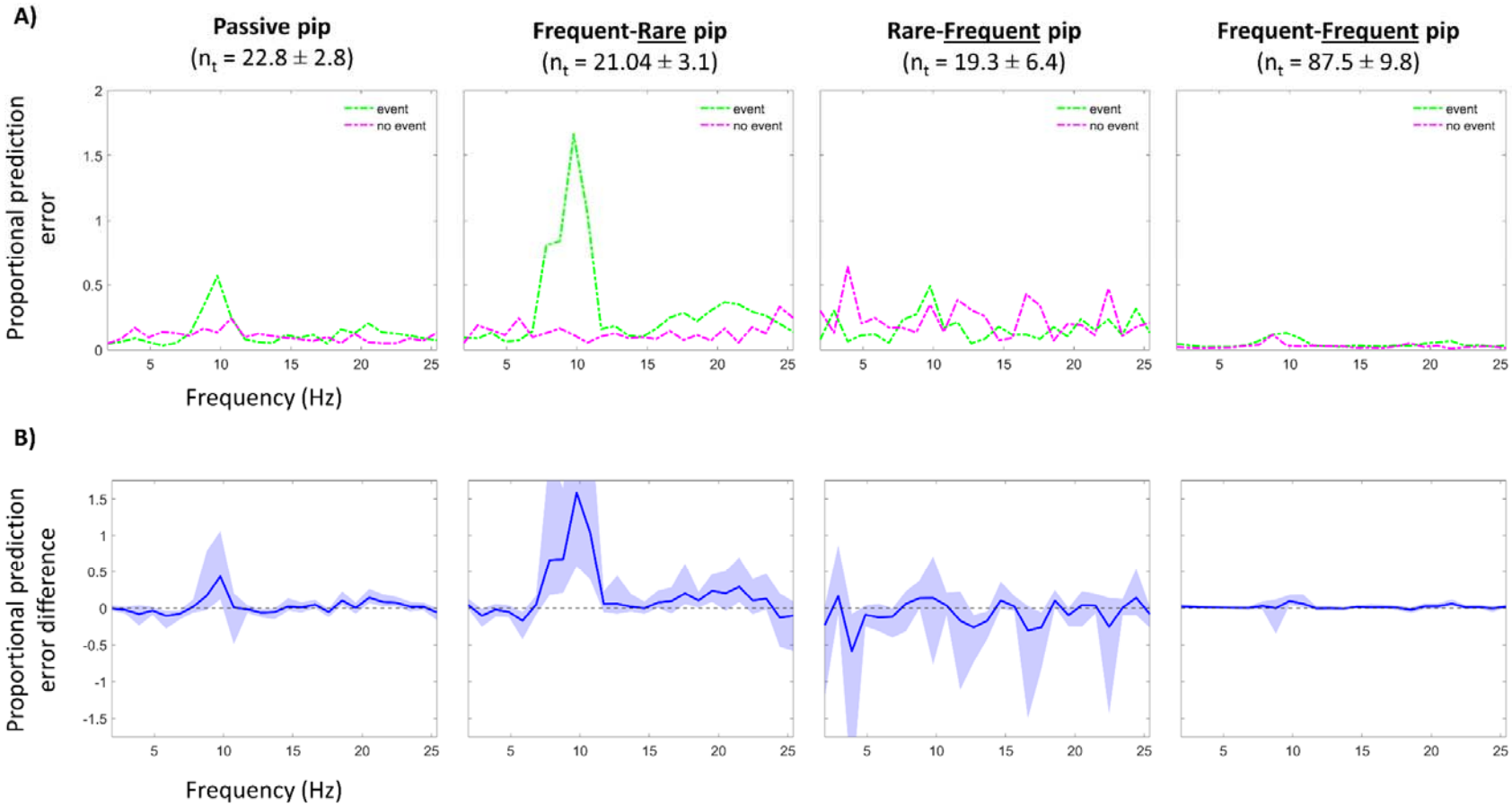
A)
Passive pip
($n_t$ = 22.8 ± 2.8)
Frequent-Rare pip
($n_t$ = 21.04 ± 3.1)
Rare-Frequent pip
($n_t$ = 19.3 ± 6.4)
Frequent-Frequent pip
($n_t$ = 87.5 ± 9.8)
event
no event
Proportional prediction error
Frequency (Hz)
B)
Proportional prediction error difference
Frequency (Hz)

460
461

**Figure 5** – Frequency-wise proportional prediction errors across different conditions. Trial numbers differ across conditions, $n_t$ = mean trial numbers ± SD. A) Proportional prediction errors using the two-predictor model. The event line (green) is identical to the green line in Fig. 3A, and reflects unexplained variance in the post-event spectrum when using the pre-event (event-1) spectrum and the spectrum of the ERPs as predictors. The no event line (magenta) reflects unexplained variance in the pre-event (event-1) spectrum when using the event-2 spectrum and the spectrum of the time-domain averaged activity in the pre-event (event-1) time window (pseudo-ERP). Values are averaged across individuals. B) The difference between the event and the no event error curves (the green and magenta lines from Row A, respectively). Shading is 95% bootstrapped confidence interval.

In summary, our findings suggest that, with the exception of alpha suppression, post-event spectral changes in the present data, i.e., in the case of simple auditory stimulation conditions, can be modelled as the sum of the pre-event spectrum and the spectrum of the ERP, at least within the error of measurement.

## 4. Discussion

In the present study, we investigated event-related changes in non-oscillatory activity in the brain during two simple auditory tasks, focusing especially on 1/*f* activity across time. We found a set of complex changes in the spectral composition of neural activity in response to auditory stimuli in our datasets. Importantly, in addition to expected post-event changes in oscillatory activity such as alpha suppression (e.g., Feng et al., 2017; Foxe & Snyder, 2011; Klimesch, 1999; Klimesch et al., 2007; Palva & Palva, 2007), apparent changes in both the offset and the slope of 1/*f*-like, aperiodic activity (as estimated using the FOOOF algorithm, (Donoghue et al., 2020)) were also consistently observed across tasks. However, this spectral shift from before to after stimulation was satisfactorily accounted for by the presence of transient activity, time locked to the events: in other words, by the presence of ERPs, as opposed to reflecting changes induced in ongoing background activity.

Specifically, we found that low frequency activity in the power spectrum of neural signals immediately following an auditory stimulus can be modelled quite accurately (i.e., within the measurement error) as a sum of pre-event spectral content, largely characterized by a 1/*f*-like pattern, and the spectral content of the ERPs elicited by the stimulus (for a similar additive framework see Gyurkovics et al., 2021). In the delta and theta ranges, the variance unaccounted for by this simple two-predictor model was not substantially larger than the unexplained variance when the spectral content of 1 second of activity was used to predict the spectral content of the following second, in the absence of any event, i.e., when the

unexplained variance merely captures random, moment-to-moment variability in the signal. Importantly, this pattern was observed across two different tasks, a simple passive auditory perception task with no top-down attentional requirements and an auditory oddball task with an attentional load. These findings suggest that while the shape of 1/*f*-like background activity does appear to change from before an event to immediately after an event, these apparent changes in the offset and exponent of aperiodic activity are due to the emergence of transient, event-related activity, while ongoing non-oscillatory activity – which the 1/*f* curve is thought to capture (Donoghue et al., 2020; He, 2014) – may remain unchanged in its temporospatial characteristics.

Although the observations described above held for most frequencies, the two-predictor model (based on the sum of pre-event spectral content and the spectrum of the ERP) did not have good predictive power in the alpha range. This is likely because, as noted above, alpha oscillations were *suppressed* following the onset of the stimulus compared to the pre-event time window. This suppression could not be accounted for by adding the power spectrum of the ERP on top of the pre-event activity because power is a squared measure and cannot take negative values. Therefore, this model cannot account for post-stimulus dips in power at any frequency. In general, it is also worth noting that the ERP spectrum contained no clear peak in the alpha range in most conditions, above and beyond the power law scaling of the spectrum, suggesting that these midfrontal ERPs likely did not arise from alpha oscillations becoming phase-locked to the stimulus (see a different model for posterior visual ERPs, Makeig et al., 2002).

Interestingly, a bump in the theta frequency range was observed in some conditions in the spectrum of the ERP – and relatedly, in the post-event power spectrum -, but never in the pre-event spectra (for more on theta effects in the current data set, see Clements, Gyurkovics, et al., 2021)). This observation and the high predictive power of the two-predictor model in

the theta range suggests that, at least in these perceptual and attention tasks, midfrontal theta activity was completely elicited by, and phase-locked to, the task stimuli, and did not reflect an ongoing oscillation present between trials whose phase or amplitude could change in response to the occurrence of the target stimuli (as proposed in Cohen, 2014a; Cohen & Donner, 2013). This contrasts with the behavior of alpha oscillations, which, as noted above, were clearly present before the target stimuli, were not phase-reset by the event, and decreased in their amplitude when a tone was presented. In other words, theta activity was elicited by the stimulus, whereas alpha suppression was induced by the stimulus (Cohen, 2014b; Herrmann et al., 2014; Pfurtscheller & Da Silva, 1999). These observations are supported by traditional phase-locking analyses, presented in the supplementary materials (Supp. Fig. 4), which reveal transient inter-trial phase clustering only in frequencies below the alpha range in our data.

Finally, at frequencies above the alpha range, a single-predictor model, which predicted post-event spectral changes based on pre-event spectral content alone, occasionally outperformed the two-predictor model (e.g., in the frequent-rare condition, see Fig. 4). The relatively poorer performance of the summation-based two-predictor model at higher frequencies is likely because the spectrum of the ERP contains no real signal at these frequencies, due to the low-pass filtering nature of time-domain averaging. Time-domain averaging, a necessary step in the calculation of ERPs, eliminates high frequency activity, which is less likely to summate across trials. As such, the two-predictor model considers high frequencies as a sum of pre-event activity and random noise (the contribution of the ERP spectrum), making its estimates noisier than those of the single-predictor model, which does not contain the additional noise component. Notably, the low-pass filtering inherent in the calculation of ERPs also explains why the average ERP spectra show a decrease in power across frequencies, as can be observed in Fig. 3.

### 4.1 Theoretical and methodological implications

Most previous studies that did find evidence for event-related changes in the shape – typically, the slope – of ongoing 1/*f* activity used intracranial recordings (Miller et al., 2009; Podvalny et al., 2015). It is, however, quite plausible that 1/*f*-like activity in intracranial recordings (micro- or meso-scale) and 1/*f*-like activity in non-invasive surface recordings (macro-scale) reflect different generative mechanisms, and therefore, cannot be expected to behave similarly across similar manipulations or situations. While the 1/*f*-like pattern of power spectra in the former case might be related to the decay time of post-synaptic potentials (Voytek & Knight, 2015), in M/EEG surface recordings the spatial summation of activity necessary to generate a measurable signal might be sufficient to account for the power law scaling of the spectrum. In addition to being less likely to summate across time, high frequency activity is also less likely to summate across space. As such, spatial summation may act as a low-pass spatial filter similarly to time-domain averaging, resulting in a 1/*f*-like pattern in signals measured non-invasively. Therefore, any findings based on surface level recordings concerning the functional significance of 1/*f*-like activity (Wainio-Theberge et al., 2021; Waschke et al., 2021) may be capturing changes in low frequency activity, which may partly be due to the emergence of ERPs (although see control analyses in Waschke et al., 2021).

Notably, this possibility does not invalidate the popular account which posits that changes in the shape of 1/*f* activity reflect changes in the balance of excitatory and inhibitory neural inputs, regardless of the invasiveness of the recording (Gao et al., 2017; Waschke et al., 2021), given that activity elicited by an event (ERP) arguably – and trivially – also reflects a shift in the balance of excitation and inhibition in neural populations. Our findings, however, increase the explanatory power of this account by suggesting that 1/*f*-like scaling in the frequency domain of a signal might reflect a combination of stimulus-related and

stimulus-unrelated (ongoing, background) activities that are both non-oscillatory in nature (i.e., they do not include ongoing alpha oscillations). Importantly, failing to disentangle these factors contributing to the shape of the power spectrum could lead to erroneous conclusions regarding the mechanisms generating neural signals. Specifically, in our datasets, we observed a general steepening of 1/*f* activity from pre- to post-event, which would normally be interpreted as a shift towards inhibitory as opposed to excitatory activity (Colombo et al., 2019; Gao et al., 2017; Lendner et al., 2020; Miskovic et al., 2019; Waschke et al., 2021). However, our subsequent analyses indicate that it would be premature to conclude that auditory stimuli lead to increased inhibition. In fact, the change in the shape of the power spectrum may instead simply reflect relatively unchanged background activity with the addition of low-frequency components, in the form of ERPs, which then bias the estimation of the offset and the exponent of aperiodic activity towards larger absolute values (see Gerster et al., 2021, who articulate a similar caveat for spectral analysis, albeit focusing on the impact of low-frequency oscillations).

Our findings have methodological implications as well. First and foremost, we suggest that researchers interested in event-related changes in the spectral content of neural activity, including 1/*f* activity, utilize paradigms with ITIs long enough (~1024 ms or preferably more) to provide good frequency resolution on both sides of the target stimulus, and then contrast the pre- and post-event power spectra directly, as was done here. This avoids the temporal and frequency smearing inherent in traditional time-frequency analysis, and therefore enables the uncontaminated estimation of ongoing (pre-stimulus) and post-stimulus activity. It is also advisable to investigate the spectrum of the ERPs elicited by the stimulus, a step rarely done in the literature. This provides researchers with a fast and computationally uninvolved way to examine which spectral changes are phase-locked and which are not. Crucially, it can be

subtracted or regressed out of the post-event spectrum, to recover changes induced in ongoing activity by the stimulus, if there are any.

When the research question concerns the timing or duration of spectral - typically oscillatory - changes, time-frequency analysis is a more advantageous analytic choice due to its superior temporal resolution. As noted in the Introduction, this technique usually involves baseline subtraction or division as a means of separating oscillatory changes from 1/*f* activity (Cohen, 2014b; Gyurkovics et al., 2021; Herrmann et al., 2014). Baseline correction assumes that 1/*f* activity does not change from the baseline period (typically the pre-event period) to the post-event period, therefore removing an estimate of the former from the latter will recover only event-related changes. Our findings largely support this assumption, with one important caveat: what is likely to be recovered this way is not purely oscillatory activity, but will also include ERPs, which have a broadband representation in the frequency domain. This could lead to a misinterpretation of any changes in the lower frequencies because these changes may not, in fact, be due to a shift in low frequency oscillations, but rather to changes in non-oscillatory processes. Consequently, researchers need to be careful when interpreting baseline-corrected low frequency (i.e., below alpha range) activity in time-frequency analysis.

Finally, our data also indirectly address the issue of phase-resetting of ongoing oscillations as a possible mechanism for the generation of ERPs. The present findings provide no clear evidence for this phenomenon, at least within our tasks. For a specific frequency, a pattern indicative of phase resetting would be the observation of no change in power in the post-event spectrum compared to the pre-event spectrum, and a clear peak in the spectrum of the ERP, leading to under-additivity of the pre-stimulus and ERP spectra in generating the post-stimulus spectrum. For no frequency did we observe the presence of both phenomena concurrently. At frequencies below alpha, power increased after stimulation rather than remaining constant, and the two-predictor model accurately predicted the observed post-

stimulus power. In the alpha band, power decreased after stimulation (but see below for a possible caveat for this statement). At frequencies above alpha, there was relatively little power in the spectrum of ERP waveforms, again inconsistent with phase resetting. One further challenge for phase-resetting as a general mechanism for ERP generation is that only true oscillatory activity has an interpretable phase, which can then be reset; aperiodic activity, by definition, is not oscillatory and therefore its phase is undefined. However, our analyses indicate that, apart from alpha, no other true oscillatory activity can be consistently identified in the pre-stimulus EEG activity. Therefore, the only oscillatory EEG activity that could be reset by the presentation of a stimulus, so as to produce an ERP, would be alpha activity.

A limitation of our conclusions about possible resetting mechanisms for alpha is that the temporal resolution of our frequency-domain analysis was very low, as information was integrated over periods of about 1 second. This was done to ensure adequate frequency resolution for our main analyses. However, it is still possible for high-frequency oscillatory activity of short duration (i.e., not longer than a few hundred milliseconds) to be missed by this approach, along with short-duration phase-resetting episodes. Importantly, however, episodes of such a short duration are hardly compatible with oscillations occurring at low frequencies. Thus, by-and-large the data do not provide clear support for a contribution of phase-resetting mechanisms to the generation of scalp-recorded ERP activity, at least for auditory stimulation.

### 4.2 Conclusions

In the present study, we investigated event-related changes in non-oscillatory neural activity using EEG in two auditory tasks. We found that while the offset and slope of 1/*f*-like non-oscillatory activity do appear to increase in the post-event time window compared to the pre-event time window, these apparent changes were largely explained by the emergence of

ERPs, that is, by the non-oscillatory activity elicited by the event. Post-event activity could be modelled as the sum of pre-event activity and the ERP spectrum, except in the alpha range where true induced oscillatory changes could be observed. In short, we found no evidence for induced changes in non-oscillatory activity, only in stimulus-elicited non-oscillatory signals. Future studies are needed with more complex cognitive manipulations to test the generalizability of these findings, and to investigate more closely whether changes in midfrontal theta power are typically elicited, induced, or both. Furthermore, we caution researchers regarding the interpretation of low-frequency activity changes in baseline-corrected time-frequency domain data.

**Acknowledgments**

This work was supported by NIA grant RF1AG062666 to G. Gratton and M. Fabiani.

## References


Acharya, J. N., Hani, A. J., Cheek, J., Thirumala, P., & Tsuchida, T. N. (2016). American clinical neurophysiology society guideline 2: guidelines for standard electrode position nomenclature. *The Neurodiagnostic Journal*, *56*(4), 245–252.

Başar, E., Başar-Eroğlu, C., Karakaş, S., & Schürmann, M. (2000). Brain oscillations in perception and memory. *International Journal of Psychophysiology*, *35*(2–3), 95–124. https://doi.org/10.1016/S0167-8760(99)00047-1

Bódizs, R., Szalárdy, O., Horváth, C., Ujma, P. P., Gombos, F., Simor, P., Pótári, A., Zeising, M., Steiger, A., & Dresler, M. (2021). A set of composite, non-redundant EEG measures of NREM sleep based on the power law scaling of the Fourier spectrum. *Scientific Reports*, *11*(1), 1–18.

Brumback, C. R., Low, K. A., Gratton, G., & Fabiani, M. (2005). Putting things into perspective: Individual differences in working-memory span and the integration of information. *Experimental Psychology*, *52*(1), 21–30.

Buzsáki, G. (2002). Theta oscillations in the hippocampus. *Neuron*, *33*(3), 325–340. https://doi.org/10.1016/S0896-6273(02)00586-X

Clayton, M. S., Yeung, N., & Kadosh, R. C. (2015). The roles of cortical oscillations in sustained attention. *Trends in Cognitive Sciences*, *19*(4), 188–195. https://doi.org/10.1016/j.tics.2015.02.004

Clements, G. M., Bowie, D. C., Gyurkovics, M., Low, K. A., Fabiani, M., & Gratton, G. (2021). Spontaneous alpha oscillations and low-frequency activities are related to complementary aspects of cognitive control in younger and older adults. *Frontiers in Human Neuroscience*, *15*. https://doi.org/10.3389/fnhum.2021.621620

Clements, G. M., Gyurkovics, M., Low, K. A., Beck, D. M., Fabiani, M., & Gratton, G. (2021). Dynamics of alpha suppression and enhancement may be related to resource

competition in cross-modal cortical regions. *BioRxiv*. https://doi.org/10.1101/2021.11.29.470447

Cohen, M. X. (2014a). A neural microcircuit for cognitive conflict detection and signaling. *Trends in Neurosciences*, *37*(9), 480–490. https://doi.org/10.1016/j.tins.2014.06.004

Cohen, M. X. (2014b). Analyzing Neural Time Series Data. In *Analyzing Neural Time Series Data*. MIT Press. https://doi.org/10.7551/mitpress/9609.001.0001

Cohen, M. X., & Donner, T. H. (2013). Midfrontal conflict-related theta-band power reflects neural oscillations that predict behavior. *Journal of Neurophysiology*, *110*(12), 2752–2763. https://doi.org/10.1152/jn.00479.2013

Colombo, M. A., Napolitani, M., Boly, M., Gosseries, O., Casarotto, S., Rosanova, M., Brichant, J.-F., Boveroux, P., Rex, S., & Laureys, S. (2019). The spectral exponent of the resting EEG indexes the presence of consciousness during unresponsiveness induced by propofol, xenon, and ketamine. *Neuroimage*, *189*, 631–644.

Donoghue, T., Haller, M., Peterson, E., Varma, P., Sebastian, P., Gao, R., Noto, T., Lara, A. H., Wallis, J. D., Knight, R. T., Shestyuk, A., & Voytek, B. (2020). Parameterizing neural power spectra into periodic and aperiodic components. *Nature Neuroscience*. https://doi.org/10.1038/s41593-020-00744-x

Feng, W., Störmer, V. S., Martinez, A., McDonald, J. J., & Hillyard, S. A. (2017). Involuntary orienting of attention to a sound desynchronizes the occipital alpha rhythm and improves visual perception. *NeuroImage*, *150*, 318–328.

Foxe, J. J., & Snyder, A. C. (2011). The role of alpha-band brain oscillations as a sensory suppression mechanism during selective attention. *Frontiers in Psychology*, *2*, 154.

Gao, R., Peterson, E. J., & Voytek, B. (2017). Inferring synaptic excitation/inhibition balance from field potentials. *Neuroimage*, *158*, 70–78.

Gerster, M., Waterstraat, G., Litvak, V., Lehnertz, K., Schnitzler, A., Florin, E., Curio, G., &

Nikulin, V. (2021). Separating neural oscillations from aperiodic 1/f activity: challenges and recommendations. *BioRxiv*.

Gratton, G. (2018). Brain reflections: A circuit based framework for understanding information processing and cognitive control. *Psychophysiology*, *55*(3), e13038. https://doi.org/10.1111/psyp.13038

Gratton, G., Coles, M. G. H., & Donchin, E. (1983). A new method for off-line removal of ocular artifact. *Electroencephalography and Clinical Neurophysiology*, *55*(4), 468–484. https://doi.org/10.1016/0013-4694(83)90135-9

Gyurkovics, M., Clements, G. M., Low, K. A., Fabiani, M., & Gratton, G. (2021). The impact of 1/f activity and baseline correction on the results and interpretation of time-frequency analyses of EEG/MEG data: A cautionary tale. *NeuroImage*, 118192.

He, B. J. (2014). Scale-free brain activity: past, present, and future. *Trends in Cognitive Sciences*, *18*(9), 480–487. https://doi.org/10.1016/j.tics.2014.04.003

He, B. J., Zempel, J. M., Snyder, A. Z., & Raichle, M. E. (2010). The temporal structures and functional significance of scale-free brain activity. *Neuron*, *66*(3), 353–369. https://doi.org/10.1016/j.neuron.2010.04.020

Herrmann, C. S., Rach, S., Vosskuhl, J., & Strüber, D. (2014). Time–frequency analysis of event-related potentials: a brief tutorial. *Brain Topography*, *27*(4), 438–450. https://doi.org/10.1007/s10548-013-0327-5

Immink, M. A., Cross, Z. R., Chatburn, A., Baumeister, J., Schlesewsky, M., & Bornkessel-Schlesewsky, I. (2021). Resting-state aperiodic neural dynamics predict individual differences in visuomotor performance and learning. *Human Movement Science*, *78*, 102829.

Jasper, H. (1958). Report of the committee on methods of clinical examination in electroencephalography. *Electroencephalogr Clin Neurophysiol*, *10*, 370–375.

Klimesch, W. (1999). EEG alpha and theta oscillations reflect cognitive and memory performance: a review and analysis. *Brain Research Reviews*, *29*(2–3), 169–195.

Klimesch, W., Sauseng, P., & Hanslmayr, S. (2007). EEG alpha oscillations: the inhibition–timing hypothesis. *Brain Research Reviews*, *53*(1), 63–88.

Lendner, J. D., Helfrich, R. F., Mander, B. A., Romundstad, L., Lin, J. J., Walker, M. P., Larsson, P. G., & Knight, R. T. (2020). An electrophysiological marker of arousal level in humans. *Elife*, *9*, e55092.

Luck, S. J. (2014). *An introduction to the event-related potential technique*. MIT press.

Lundqvist, M., Rose, J., Herman, P., Brincat, S. L., Buschman, T. J., & Miller, E. K. (2016). Gamma and beta bursts underlie working memory. *Neuron*, *90*(1), 152–164. https://doi.org/10.1016/j.neuron.2016.02.028

Makeig, S., Westerfield, M., Jung, T.-P., Enghoff, S., Townsend, J., Courchesne, E., & Sejnowski, T. J. (2002). Dynamic brain sources of visual evoked responses. *Science*, *295*(5555), 690–694. https://doi.org/10.1126/science.1066168

Mathewson, K. E., Lleras, A., Beck, D. M., Fabiani, M., Ro, T., & Gratton, G. (2011). Pulsed out of awareness: EEG alpha oscillations represent a pulsed-inhibition of ongoing cortical processing. *Frontiers in Psychology*, *2*, 99. https://doi.org/10.3389/fpsyg.2011.00099

Miller, K. J., Sorensen, L. B., Ojemann, J. G., & Den Nijs, M. (2009). Power-law scaling in the brain surface electric potential. *PLoS Comput Biol*, *5*(12), e1000609. https://doi.org/10.1371/journal.pcbi.1000609

Min, B.-K., Busch, N. A., Debener, S., Kranczioch, C., Hanslmayr, S., Engel, A. K., & Herrmann, C. S. (2007). The best of both worlds: phase-reset of human EEG alpha activity and additive power contribute to ERP generation. *International Journal of Psychophysiology*, *65*(1), 58–68.

Mishra, J., Martínez, A., Schroeder, C. E., & Hillyard, S. A. (2012). Spatial attention boosts short-latency neural responses in human visual cortex. *Neuroimage*, *59*(2), 1968–1978.

Miskovic, V., MacDonald, K. J., Rhodes, L. J., & Cote, K. A. (2019). Changes in EEG multiscale entropy and power□law frequency scaling during the human sleep cycle. *Human Brain Mapping*, *40*(2), 538–551.

Ouyang, G., Hildebrandt, A., Schmitz, F., & Herrmann, C. S. (2020). Decomposing alpha and 1/f brain activities reveals their differential associations with cognitive processing speed. *NeuroImage*, *205*, 116304. https://doi.org/10.1016/j.neuroimage.2019.116304

Palva, S., & Palva, J. M. (2007). New vistas for α-frequency band oscillations. *Trends in Neurosciences*, *30*(4), 150–158.

Pfurtscheller, G., & Da Silva, F. H. L. (1999). Event-related EEG/MEG synchronization and desynchronization: basic principles. *Clinical Neurophysiology*, *110*(11), 1842–1857.

Podvalny, E., Noy, N., Harel, M., Bickel, S., Chechik, G., Schroeder, C. E., Mehta, A. D., Tsodyks, M., & Malach, R. (2015). A unifying principle underlying the extracellular field potential spectral responses in the human cortex. *Journal of Neurophysiology*, *114*(1), 505–519. https://doi.org/10.1152/jn.00943.2014

Pritchard, W. S. (1992). The brain in fractal time: 1/f-like power spectrum scaling of the human electroencephalogram. *International Journal of Neuroscience*, *66*(1–2), 119–129.

Sauseng, P., Klimesch, W., Gruber, W. R., Hanslmayr, S., Freunberger, R., & Doppelmayr, M. (2007). Are event-related potential components generated by phase resetting of brain oscillations? A critical discussion. *Neuroscience*, *146*(4), 1435–1444. https://doi.org/10.1016/j.neuroscience.2007.03.014

Voytek, B., & Knight, R. T. (2015). Dynamic network communication as a unifying neural basis for cognition, development, aging, and disease. *Biological Psychiatry*, *77*(12), 1089–1097. https://doi.org/10.1016/j.biopsych.2015.04.016

Wainio-Theberge, S., Wolff, A., & Northoff, G. (2021). Dynamic relationships between spontaneous and evoked electrophysiological activity. *Communications Biology*, *4*(1), 1–17.

Waschke, L., Donoghue, T., Fiedler, L., Smith, S., Garrett, D. D., Voytek, B., & Obleser, J. (2021). Modality-specific tracking of attention and sensory statistics in the human electrophysiological spectral exponent. *Elife*, *10*, e70068. https://doi.org/10.7554/eLife.70068